Optical Phased Array on Silicon Photonic Platform

Jie Sun*, Ami Yaacobi, Erman Timurdogan, Ehsan Shah Hosseini,
Douglas Coolbaugh, Gerald Leake, and Michael R. Watts

***Abstract*—Large-scale optical phased arrays containing up to 64×64 nanoantennas are demonstrated on silicon photonic platform, representing the largest scale demonstrated to date. Active phase tuning is also realized for dynamic pattern generation.**

***Keywords*—Integrated Optics, Silicon Photonics**

I. Introduction

OPTICAL phased arrays are promising for a broad range of applications such as Laser Detection And Ranging (LADAR), optical free-space communication, holographic displays, optical trapping, *etc*. To enable these applications, it is essential to integrate a large number of antennas on a compact platform to increase the far-field resolution. Although integrated optical phased arrays have been well studied [1] [2], all of the demonstrations are limited to 1-dimensional (1-D) or small-scale 2-dimensional (2-D) arrays containing no more than 16 antennas. Here we present large-scale integrated optical phased arrays on the silicon photonic platform enabled by the state-of-the-art Complementary Metal-Oxide-Semiconductor (CMOS) technology [3]. Two passive phased arrays, 64×64 and 32×32, are shown to create sophisticated holographic images in the far field, as well as an 8×8 active phased array that is capable of dynamically shaping the optical beam through thermo-optic tuning of the antenna phase, representing the largest and most complex optical phased arrays demonstrated to date.

II. Passive Phased Array

Figure 1(a) shows the structure of a large-scale ($N \times N$) passive phased array on the silicon photonic platform. An optical input at 1.55μm is launched from a fiber to a silicon bus waveguide which is then evanescently coupled into N silicon row waveguides through the directional couplers. Light in each row waveguide is subsequently coupled to N unit cells. The coupling efficiency is varied by accurately adjusting the length of each directional coupler (L_{mn}) so as to have each unit cell emit the same optical power. As shown in Fig. 1(b), each unit cell contains an efficient silicon grating emitter as an optical nanoantenna and a waveguide delay line to precisely allocate the desired optical phase φ_{mn} to each emitter. By assigning each antenna unit in the phased array with a specific optical phase which could be calculated by the Gerchberg-Saxon algorithm [4], complex patterns can be holographically formed in the far field, as shown by the simulations in Fig. 2(b) where an MIT-logo is created and in Fig. 2(c) where a pattern with 9 beams aligned in a concentric way is generated. Multiple interference orders are seen in the far field, which is a consequence of a larger antenna spacing (9μm×9μm) compared to the wavelength used.

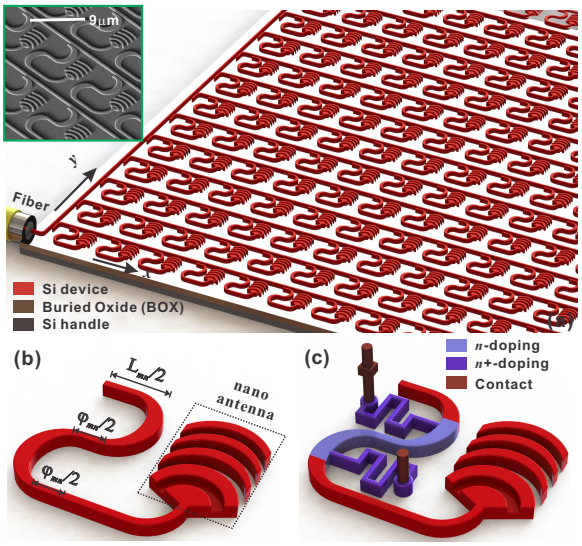

Fig. 1. (a) A schematic of the large-scale optical phased array on the silicon photonic platform. Inset: an SEM of the fabricated phased array. (b) A schematic of a passive unit cell with designed coupling length L_{mn} and phase delay φ_{mn}. (c) A schematic of an active unit cell with integrated thermo-optic phase tunability.

The phased array is fabricated in a 300-mm CMOS foundry with 193-nm optical immersion lithography at 65-nm technology node. Silicon-on-insulator (SOI) with 220nm device layer and 2μm buried oxide (BOX) is used. A full silicon etch and a partial silicon etch (110nm) are performed to define the waveguide and nanoantennas. The inset of Fig. 1(a) shows a scanning-electron-micrograph (SEM) of the fabricated passive phased array. Figure 2(a) shows the near-field emission of a 64×64 phased array where uniform emission is observed across all of the 4,096 nanoantennas. Figure 2(d) measures the far-field image generated by a 64×64 array showing the MIT-logo. Another 32×32 array creates a far-field pattern corresponding to that in Fig. 2(c), as shown in Fig. 2(e). The measurements agree well with the simulation results, confirming the robustness of the design and reliability of the CMOS fabrication. This unique ability to generate arbitrary far-field patterns enabled by the large-scale phased array with the state-

J. Sun, A. Yaacobi, E. Timurdogan, E. S. Hosseini and M. R. Watts are with the Research Laboratory of Electronics, Massachusetts Institute of Technology, Cambridge, MA 02139, USA e-mail: sunjie@mit.edu.

G. Leake and D. Coolbaugh are with the College of Nanoscale Science & Technology, University at Albany, State University of New York, Albany, NY 12203, USA

of-the-art CMOS technology could find potential applications in optical beam shaping, holography, optical trapping, *etc.*

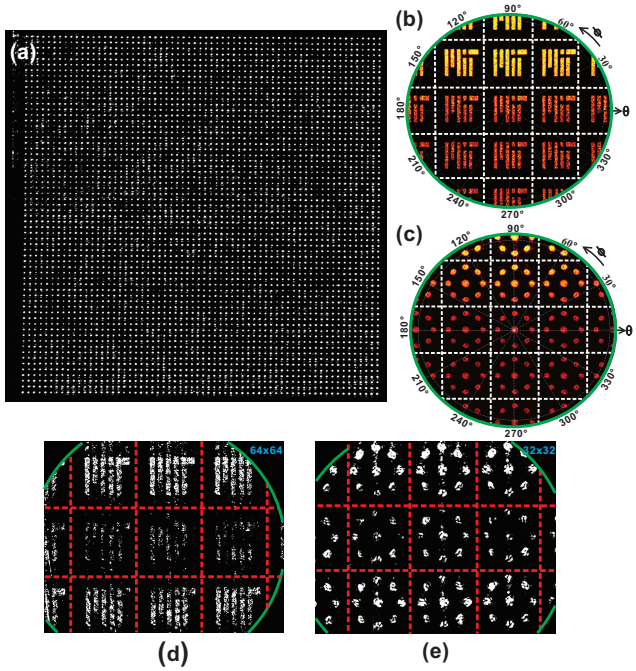

Fig. 2. (a) Uniform near-field emission from a 64×64 optical phased array. Simulated far-field patterns of (b) the MIT-logo generated from a 64×64 array, and (c) a concentric ring pattern created by a 32×32 array. Multiple interference orders are seen. Measured far-field images showing (d) the MIT-logo and (e) the pattern with multiple beams aligned in a concentric way.

III. Active Phased Array

Although many applications could be found in passive phased arrays, active phased arrays are more appealing owing to its ability to dynamically shape the optical beams. To this end, ultra-compact active phase shifter needs to be integrated in each antenna unit cell for dynamic phase tuning. This is achieved by a thermo-optic silicon heater intimately integrated in each antenna unit cell by slightly doping the silicon waveguide to form a resistor [5], as shown in Fig. 1(c). By applying voltages on the heater, the phase of the optical emission from each nanoantenna can be tuned from 0 to 2π. Figures 3(a)-(g) show versatile far-field patterns generated by an 8×8 phased array by applying different voltage configurations to the phased array, where the original focused optical beam (Fig. 3(a)) can be steered (Fig. 3(b) and (c)), split into 2 beams (Fig. 3(d) and (e)), and into 4 beams (Fig. 3(f) and (g)) in vertical and horizontal directions. In spite of the smaller scale of the active phased array compared to the passive demonstrations which is limited by the electrical connectivity in our fabrication process, this 8×8 active phased array still represents the largest 2D active phased array demonstrated to date, and is seen as an enabling technology to applications such as LADAR, optical switching, optical coherence tomography (OCT), *etc*. With the aide of a CMOS circuitry to address and control the voltage applied to each antenna unit, the active phased array can be extended well beyond the current 8×8 case to include thousands or even million of antennas so as to dynamically project complex 3D images in the far field, a possible pathway to a truly 3D holographic display.

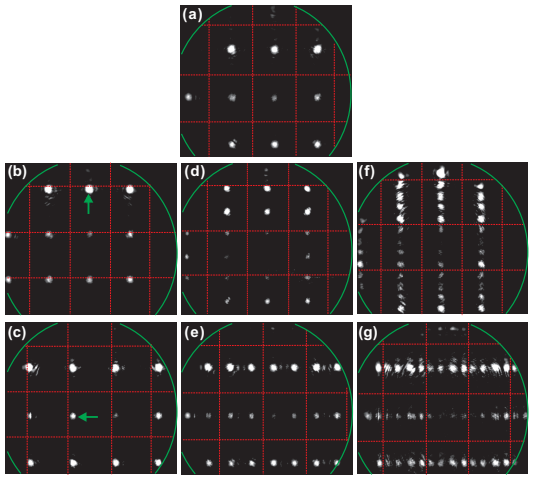

Fig. 3. (a) The original focused beam created by an 8×8 array without voltage on. The beam is steered in (b) vertical and (c) horizontal direction. The single beam is split into 2 beams in (d) vertical and (e) horizontal direction. The single beam is split into 4 beams in (f) vertical and (g) horizontal direction.

IV. Conclusion

Silicon photonics combined with the well-established CMOS fabrication technology, large-scale optical phased arrays are demonstrated with the ability to project sophisticated and dynamic patterns in the far field, representing the largest and most complex optical phased array demonstrated to date.

Acknowledgment

This work was supported by DARPA under the E-PHI and SWEEPER projects, grant no. HR0011-12-2-0007.

References

[1] J. K. Doylend, M. J. R. Heck, J. T. Bovington, J. D. Peters, M. L. Davenport, L. A. Coldren, and J. E. Bowers, "Hybrid III/V silicon photonic source with integrated 1D free-space beam steering," *Opt. Lett.*, vol.37, no.20, pp.4257-4259, 2012

[2] K. Van Acoleyen, H. Rogier, and R. Baets, "Two-dimensional optical phased array antenna on silicon-on-insulator," *Opt. Express*, vol.18, no.13, pp.13655-13660, 2010

[3] J. Sun, E. Timurdogan, A. Yaacobi, E. S. Hosseini, and M. R. Watts, "Large-scale nanophotonic phased array," *Nature*, vol.493, no.7431, pp.195-199, 2013

[4] J. R. Fienup, "Reconstruction of an object from the modulus of its Fourier transform," *Opt. Lett.*, vol.3, no.1, pp. 2729, 1978

[5] M. R. Watts, J. Sun, C. DeRose, D. C. Trotter, R. W. Young, and G. N. Nielson, "Adiabatic thermo-optic Mach-Zehnder switch," *Opt. Lett.*, vol.38, no.5, pp.733-735, 2013